Journal of proteome research

Article

pubs.acs.org/jpr

N-Glycosylation of Serum IgG and Total Glycoproteins in MAN1B1 Deficiency

Radka Saldova,[†] Henning Stöckmann,[†] Roisin O'Flaherty,[†] Dirk J. Lefeber,[‡] Jaak Jaeken,[§] and Pauline M. Rudd*[,†]

[†]NIBRT GlycoScience Group, National Institute for Bioprocessing Research and Training, Fosters Avenue, Mount Merrion, Blackrock, Dublin 4, Ireland

[‡]Department of Neurology, Translational Metabolic Laboratory, Radboud University Medical Centre, Nijmegen, The Netherlands

[§]Centre for Metabolic Diseases, University Hospital Gasthuisberg, Leuven, Belgium

Supporting Information

ABSTRACT: MAN1B1-CDG has recently been characterized as a type II congenital disorder of glycosylation (CDG), disrupting not only protein *N*-glycosylation but also general Golgi morphology. Using our high-throughput, quantitative ultra-performance liquid chromatography assay, we achieved a detailed characterization of the glycosylation changes in both total serum glycoproteins and isolated serum IgG from ten previously reported MAN1B1-CDG patients. We have identified and quantified novel hybrid high-mannosylated MAN1B1-CDG-specific IgG glycans and found an increase of sialyl Lewis *x* (sLe*x*) glycans on serum proteins of all patients. This increase in sLex has not been previously reported in any CDG. These findings may provide insight into the pathophysiology of this CDG.

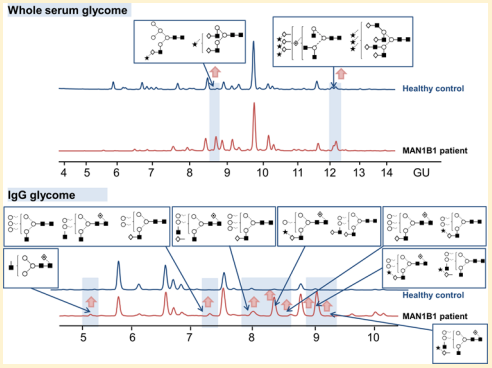

KEYWORDS: *MAN1B1, N-glycans, glycomics, ultra performance liquid chromatography, biomarkers, human serum, IgG, CDG, sialyl Lewis x*

INTRODUCTION

Glycosylation is an important post-translational modification that has a significant influence on the biological functioning of proteins. Glycoproteins are mixtures of glycosylated variants in which a protein is modified by the attachment of a heterogeneous group of glycans at glycosylation sites. Glycan processing pathways are complex and reflect the environment both within and outside of the cells. These pathways are frequently disrupted in diseases such as cancer, congenital disorders of glycosylation, and chronic inflammatory diseases, giving rise to aberrant or absent glycosylation of disease-related proteins.[1] Many glycoproteins present in human serum are key components of the native and adaptive immune system.[2] Immunoglobulins (IgGs) are important products of the humoral immune response. Human serum IgG contains two conserved *N*-linked glycosylation sites located in the Fc region at Asn297 and variable glycosylation in the Fab region of ∼20% of molecules.[3]

Congenital disorders of glycosylation (CDG) are a rapidly expanding group of genetic diseases caused by defects in the synthesis of glycoprotein and glycolipid glycans. Some 80 CDG types are actually known (see Barone et al. 2014).[4] They comprise a very broad range of phenotypes, including mostly neurological involvement.[5] CDG with abnormal *N*-glycosylation can be divided into CDG-I (defects in glycan assembly in ER) and CDG-II (defects in glycan remodelling in the Golgi). Most CDG have an autosomal-recessive inheritance; a few are transmitted as dominant or X-linked disorders.[6] The $\alpha(1,2)$-mannosidase (MAN1B1) catalyzes the removal of the terminal mannose residue from the middle branch of Man9GlcNAc2 in the Golgi, thus generating the Man8GlcNAc2 isomer B (Figure 1).[7,8] Patients with defective *MAN1B1* (MAN1B1-CDG) usually show intellectual disability, obesity, and variable dysmorphic features.[5,8,9] It is a CDG-II, and the Golgi morphology is altered in these patients' cells.[8]

Structural analysis of *N*-linked glycans on serum glycoproteins in MAN1B1-deficient patients using mass spectrometry showed an accumulation of hybrid-type glycans and some high mannose structures.[5,8] Analysis of *N*-glycans at the level of intact transferrin indicated both hybrid type *N*-glycans with one and two additional mannoses.[5] Hybrid-type *N*-glycans were also detectable in IgG and alpha1-antitrypsin in all patients investigated.[5]

Among the methods used for glycan quantitation are high performance and ultraperformance liquid chromatography (HPLC and UPLC)-HILIC with fluorescence detection linked with exoglycosidase sequencing.[10,11] In addition, several bioinformatics tools have been developed to assist the analyses, including GlycoBase, a database with HILIC, and mass spectrometry

Received: July 30, 2015
Published: September 3, 2015

DOI: 10.1021/acs.jproteome.5b00709
J. Proteome Res. 2015, 14, 4402−4412

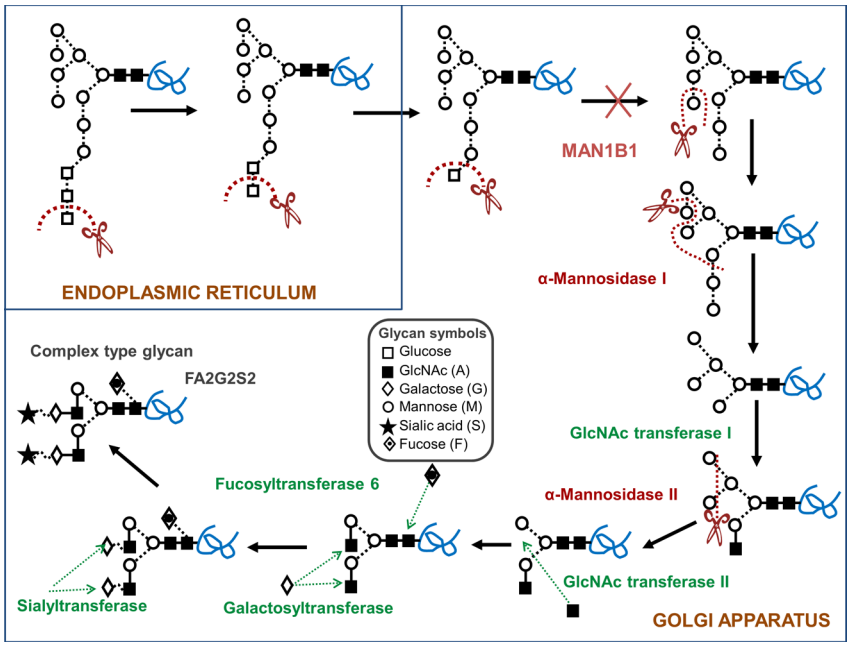

Figure 1. Location of MAN1B1 defect in the *N*-linked glycan biosynthetic pathway. Part of the affected pathway is pictured.[7,8]

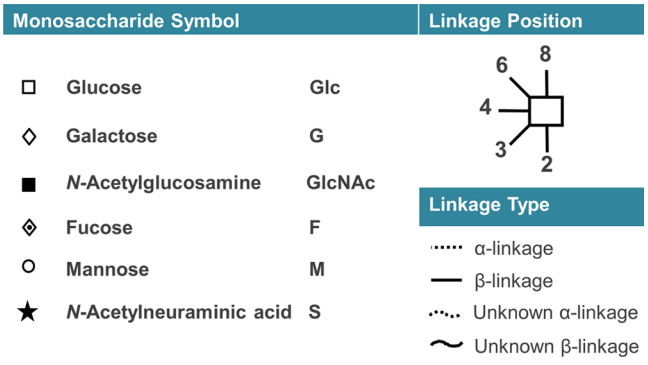

Figure 2. Glycan nomenclature.

data for 461 2-AB-labeled *N*-linked, 68 *O*-linked, and 71 free glycan structures.[11] The HPLC/UPLC analytical workflow has been automated in a robotic 96-well plate format[12,13] from sample processing through to data interpretation.

In this study, we have analyzed glycosylation of whole serum glycoproteins and serum IgG from ten previously reported MAN1B1-CDG patients using our UPLC-HILIC technology on a robotic platform to obtain a detailed overview of the glycosylation changes.

MATERIALS AND METHODS

Serum Samples

Serum was used from ten previously reported MAN1B1-CDG patients. Their phenotypes and genotypes are summarized in Supplementary Table S1. Patients 2.1 and 2.2, and 6.1 and 6.2, are siblings. A pooled serum sample (and isolated IgG from this sample) from over 100 apparently healthy male and female adult blood donors was used as a healthy control (courtesy of the UK Blood Transfusion Service).

Sample Preparation

IgG glycan sample preparation was performed on an automated glycomics platform as described in Stöckmann et al.,[12] whereby

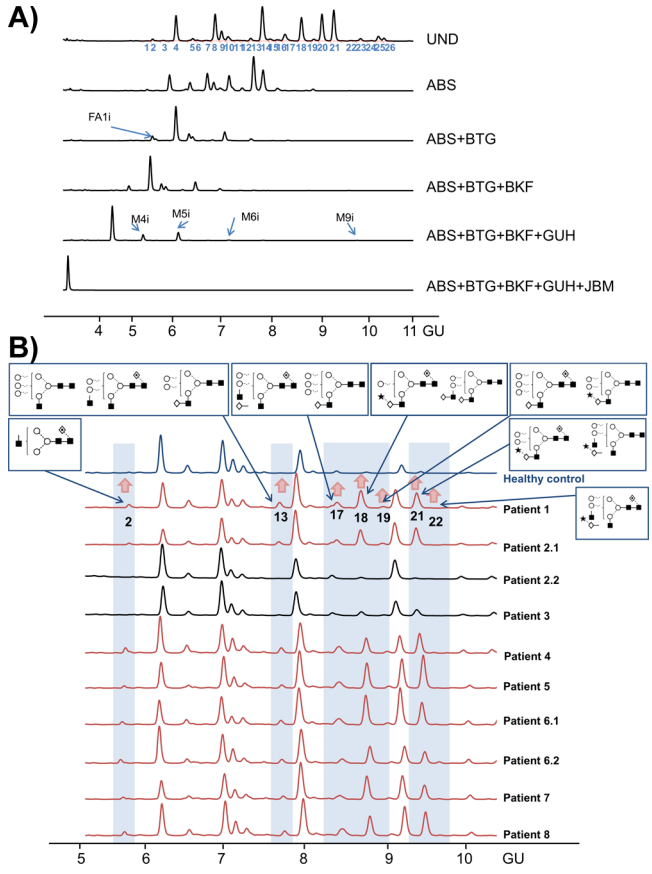

Figure 3. (A) Exoglycosidase digestions of the total *N*-linked glycan pool of IgG isolated from patient 5; specific glycans for MAN1B1-CDG are highlighted. (B) HILIC-UPLC chromatograms of the total *N*-linked glycan pool of IgG isolated from all patients. Samples are colored based on similarity (patients with similarities with the healthy control are colored in black, and patients from the two sets sharing similarities to each other are colored in red). Significantly increased peaks are highlighted with arrows, and their compositions are listed in Table 1. MAN1B1-CDG-specific glycans in major affected peaks are highlighted.

DOI: 10.1021/acs.jproteome.5b00709
J. Proteome Res. 2015, 14, 4402−4412

Table 1. *N*-Glycan Composition of 26 Peaks in Patient Serum IgG Samples[a]

Peak	Name	Structure	GU
GP1	FA1	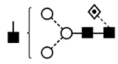	5.08
GP2	FA1i	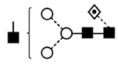	5.31
	A2		
GP3	A2B		5.48
GP4	FM4i	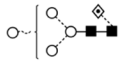	5.79
	FA2		
GP5	M5	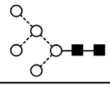	6.15
	FA1G1	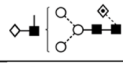	
	FA2B		
	A2[6]G1		
GP6	A2[3]G1	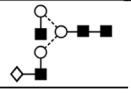	6.37
	FA1iG1	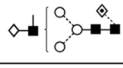	
GP7	M5iA1	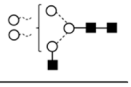	6.45
	A2BG1	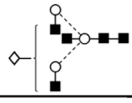	
GP8	M4iA1G1	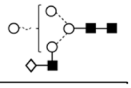	6.58
	FA2[6]G1	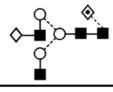	
GP9	FA2[3]G1	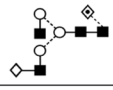	6.70
GP10	M5iA2	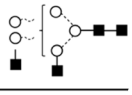	6.83
	FM5iA1	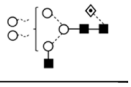	
	FA2[6]BG1		
GP11	FA2[3]BG1		6.97
	FM4iA1G1	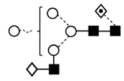	
GP12	A2G2		7.06
GP13	A2BG2	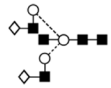	7.27
	M6iA1	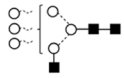	
	FM5iA2	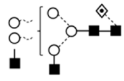	
	M5iA1G1	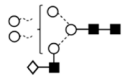	
GP14	FA2G2	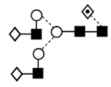	7.48
	A2G1S(6)1		
	FA1G1S(6)1	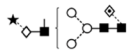	
GP15	FA1iG1S(6)1	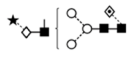	7.65
	FA2BG2		
	FM5iA1G1	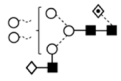	
	M5iA2G1	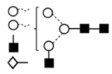	
GP16	FA2[6]G1S(6)1		7.78
	M4A1G1S(6)1	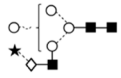	
	A2BG1S(6)1	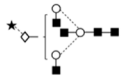	

DOI: 10.1021/acs.jproteome.5b00709
J. Proteome Res. 2015, 14, 4402−4412

Table 1. continued

Peak	Name	Structure	GU
GP17	FM5iA2G1	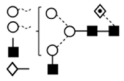	7.94
	M6iA1G1	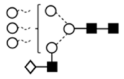	
	FA2[3]G1S(6)1	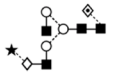	
	FA2[6]BG1S(6)1		
GP18	M5iA2G2	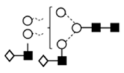	8.28
	A2G2S(6)1		
	FA2[3]BG1S(6)1	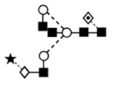	
	FM4iA1G1S(6)1	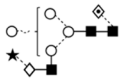	
GP19	FM6iA1G1	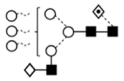	8.56
	M5iA1G1S(6)1	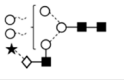	
	A2BG2S(6)1	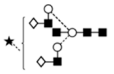	

Peak	Name	Structure	GU
GP20	FA2G2S(6)1	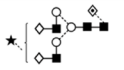	8.70
	FM5iA2G2	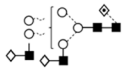	
GP21	FA2BG2S(6)1	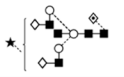	8.96
	FM5iA1G1S(6)1	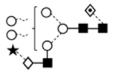	
	M5iA2G1S(6)1	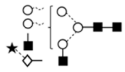	
GP22	FM5iA2G1S(6)1	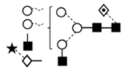	9.21
GP23	M9i	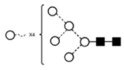	9.53
	A2G2S(6,6)2	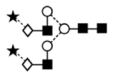	
GP24	A2BG2S(6,6)2	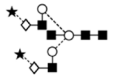	9.73
GP25	FA2G2S(6,6)2	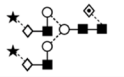	9.91
GP26	FA2BG2S(6,6)2	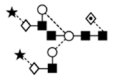	10.04
	FM5iA2G2S(6)1	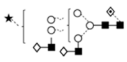	

[a]Isomer (i) of the structure. In red are highlighted glycans specific for MAN1B1-CDG on IgG and peaks containing them in major traces; GPs in red contain these specific glycans as the most abundant structures.

IgG was affinity-purified with PhyTips or Protein G plates using an updated automated serum glycomics platform described by Stöckmann et al.[13] for whole serum glycan sample preparation and analysis (see Supporting Information). Glycans were fluorescently labeled with 2-aminobenzamide (2AB) by reductive amination.[14] Samples were analyzed in duplicate.

HILIC-UPLC

HILIC-UPLC was carried out on a BEH Glycan 1.7 μM 2.1 × 150 mm column (Waters, Milford, MA) on an Acquity UPLC (Waters, Milford, MA) equipped with a Waters temperature control module and a Waters Acquity fluorescence detector. Solvent A was 50 mM formic acid adjusted to pH 4.4 with ammonia solution. Solvent B was acetonitrile. The column temperature was set to 30 °C. The following conditions were used: 30 min method using a linear gradient of 30−47% A at 0.56 mL/min in 23 min. Samples were injected in 70% acetonitrile. Fluorescence was measured at 420 nm with excitation at 330 nm. The system was calibrated using an external standard of hydrolyzed and 2AB-labeled glucose oligomers to create a dextran ladder with retention times of all identified peaks expressed as glucose units (GU), as described previously by Royle et al.[15]

Glycan Nomenclature

All *N*-glycans have two core GlcNAcs (Figure 2); F at the start of the abbreviation indicates a core $\alpha(1,6)$-fucose linked to the inner GlcNAc; M*x*, number (x) of mannose on core GlcNAcs; A*x*, number of antenna (GlcNAc) on trimannosyl core; A2, biantennary with both GlcNAcs as $\beta(1,2)$-linked; A3, triantennary with a GlcNAc linked $\beta(1,2)$- to both mannose and a third GlcNAc linked $\beta(1,4)$- to the $\alpha(1,3)$-linked mannose; A4, GlcNAcs linked as A3 with additional GlcNAc $\beta(1,6)$-linked to $\alpha(1,6)$-mannose; G*x*, number (x) of $\beta(1,4)$-linked galactose on the antenna; S*x*, number (x) of sialic acids linked to galactose; the number 3 or 6 in parentheses after S indicates whether the sialic acid is in an $\alpha(2,3)$- or $\alpha(2,6)$-linkage.

Exoglycosidase Digestion

All enzymes were purchased from Prozyme (San Leandro, CA, USA) or New England Biolabs (Ipswich, MA, USA). The 2AB-labeled glycans were digested in a volume of 10 μL for 18 h at 37 °C in 50 mM sodium acetate buffer, pH 5.5 (except in the case of jack bean α-mannosidase (JBM), where the buffer was 100 mM sodium acetate, 2 mM Zn^{2+}, pH 5.0), using arrays of the following enzymes: *Arthrobacter ureafaciens* sialidase (ABS,

DOI: 10.1021/acs.jproteome.5b00709
J. Proteome Res. 2015, 14, 4402−4412

Table 2. Percent Areas of 26 Peaks in Patient Serum IgG Samples[a]

sample	GP1	GP2	GP3	GP4	GP5	GP6	GP7	GP8	GP9	GP10	GP11
control	*0.38*	*0.72*	**1.14**	**23.55**	*5.76*	0.56	**0.90**	**20.84**	**9.06**	*5.04*	**0.85**
1	0.30	*1.16*	**0.33**	**9.87**	3.61	0.34	**0.10**	12.47	**3.74**	4.41	**0.37**
2.1	**0.07**	0.65	**0.29**	**6.52**	**2.11**	0.34	**0.07**	12.20	**3.37**	3.97	**0.18**
2.2	0.24	**0.33**	**0.44**	21.96	3.80	**0.25**	**0.13**	20.68	6.06	3.04	**0.33**
3	**0.12**	**0.32**	**0.52**	16.61	**2.72**	0.29	**0.16**	21.23	7.26	3.51	**0.37**
4	0.22	*2.24*	**0.63**	14.08	3.60	0.89	0.58	12.08	6.44	3.91	0.57
5	**0.14**	0.87	**0.49**	**10.13**	**1.43**	0.51	0.56	11.57	**4.42**	2.69	0.46
6.1	**0.16**	1.05	**0.45**	**11.38**	**2.04**	0.42	0.53	**10.29**	**3.32**	3.22	0.52
6.2	0.22	*1.72*	**0.65**	16.93	**2.29**	1.02	0.63	12.82	6.95	2.91	0.58
7	**0.15**	1.12	**0.55**	**9.32**	**1.87**	0.90	0.69	11.82	**4.77**	3.05	0.52
8	**0.16**	*1.41*	**0.60**	**11.31**	**2.40**	0.75	0.59	12.68	5.63	3.53	0.49

sample	GP12	GP13	GP14	GP15	GP16	GP17	GP18	GP19	GP20	GP21
control	*0.97*	*0.18*	15.96	*1.47*	*0.34*	*1.71*	*0.97*	*0.23*	*6.15*	*1.14*
1	0.72	*2.49*	16.41	1.50	*0.71*	*4.14*	*9.99*	*1.12*	11.60	*9.08*
2.1	0.60	*1.60*	17.73	1.66	*0.86*	*4.27*	*9.20*	*1.20*	14.69	*10.88*
2.2	0.56	0.22	14.75	0.71	*0.72*	2.91	1.25	0.18	15.02	0.87
3	**0.32**	*0.53*	16.15	1.13	0.52	2.73	*2.89*	*0.60*	10.92	*4.65*
4	0.93	*2.33*	13.71	1.44	*0.74*	*4.29*	*6.48*	*1.00*	7.64	*8.53*
5	0.56	*1.45*	15.94	1.27	*0.90*	*4.24*	*10.16*	*1.02*	11.81	*13.24*
6.1	**0.47**	*1.84*	15.26	1.43	*0.88*	*4.01*	*11.19*	*0.89*	14.31	*8.75*
6.2	0.99	*2.12*	16.53	1.23	0.66	3.19	*8.03*	*0.92*	7.93	*5.51*
7	1.12	*1.78*	18.43	1.34	*0.94*	3.24	*11.63*	*0.96*	11.98	*7.21*
8	0.77	*2.01*	15.38	1.32	*0.87*	*4.55*	*7.74*	*0.87*	11.16	*9.32*

sample	GP22	GP23	GP24	GP25	GP26
control	*0.10*	*0.66*	*0.06*	**0.61**	**0.65**
1	*0.63*	*2.16*	*0.26*	*1.53*	1.04
2.1	*0.58*	*1.74*	*0.39*	*2.76*	*2.14*
2.2	*0.28*	*2.14*	0.08	*1.98*	1.13
3	*0.21*	1.28	*0.19*	*2.60*	*2.26*
4	*0.83*	*2.01*	*0.39*	*2.20*	*2.23*
5	*0.62*	*1.38*	*0.35*	*2.39*	*1.38*
6.1	*0.85*	*1.74*	*0.39*	*2.88*	*1.71*
6.2	*1.11*	*2.28*	*0.27*	*1.40*	1.13
7	*1.00*	*2.53*	*0.42*	*1.67*	1.01
8	*0.70*	*1.58*	*0.30*	*2.20*	*1.67*

sample	G0	G1	G2	S1	S2
control	31.55	37.25	18.58	10.64	1.98
1	**15.26**	21.42	21.11	*37.26*	*4.98*
2.1	**9.62**	20.13	21.58	*41.68*	*7.02*
2.2	20.28	32.80	18.13	*22.50*	*6.31*
3	26.77	30.48	16.24	21.22	*5.32*
4	20.78	24.46	18.41	*29.51*	*6.83*
5	**13.06**	20.21	19.23	*41.99*	*5.50*
6.1	21.82	24.91	20.86	*27.33*	*5.08*
6.2	15.88	23.67	19.48	*35.22*	*5.74*
7	**13.01**	21.75	22.67	*36.95*	*5.62*
8	**15.09**	**18.31**	19.00	*40.88*	*6.72*

[a]Italics indicates more than 100% increase in percent area and bold indicates more than 100% decrease in percent area of peaks in patients compared to healthy controls. Glycans are separated based on features: nongalactosylated = G0 = GP1−5; monogalactosylated = G1 = GP6−11; digalactosylated = G2 = GP12−15; monosialylated = S1 = GP16−21; disialylated = S2 = GP23−26.

EC 3.2.1.18), 0.5 U/mL; bovine testes β-galactosidase (BTG, EC 3.2.1.23), 1 U/mL; bovine kidney α-fucosidase (BKF, EC 3.2.1.51), 1 U/mL; β-*N*-acetylglucosaminidase cloned from *S. pneumonia*, expressed in *Escherichia coli* (GUH, EC 3.2.1.30), 4 U/mL; JBM (EC 3.2.1.24), 60 U/mL; almond meal α-fucosidase (AMF, EC 3.2.1.111), 0.4 mU/mL. After incubation, enzymes were removed by filtration through 10 kDa protein-binding EZ filters (Millipore Corporation).[15] *N*-Glycans were then analyzed by UPLC.

RESULTS

N-Glycan Profiles of Serum IgG from MAN1B1-CDG Patients

Our high-throughput *N*-glycan analysis platform was utilized for IgG glycan analysis.[12] The *N*-glycan pool released from IgG was separated into 26 peaks and assigned based on exoglycosidase digestions according to Pucic et al.,[16] whereby our HILIC-UPLC technology was used to assign the IgG *N*-glycome in detail (Figure 3A, Table 1).

DOI: 10.1021/acs.jproteome.5b00709
J. Proteome Res. 2015, 14, 4402−4412

Figure 3B shows UPLC chromatograms of *N*-glycan pools from all patients compared to those of the healthy control pool. The most significant observation is that peaks GP 2, 13, 17, 18, 19, 21, and 22 (Table 1, high abundance of hybrid MAN1B1-CDG specific glycans) are significantly increased in all patients except for patient 2.2 and patient 3 (Figure 3B and Table 2) compared to those of the healthy control. These two patients have consistently lower amounts of these glycans compared to the other patients, and the amounts are almost comparable to the healthy control levels (Table 3). MAN1B1-CDG-specific glycans were quantified by digestion of the glycan pool with sialidase and β-galactosidase and with sialidase, β-galactosidase, bovine kidney α-fucosidase, and β-*N*-acetylglucosaminidase because otherwise they coelute together with other *N*-glycans in the undigested pool. The total amount was calculated from the sum of specific glycans after digestion with sialidase and β-galactosidase digest (FA1i) and specific glycans after digestion with sialidase, β-galactosidase, bovine kidney α-fucosidase, and β-*N*-acetylglucosaminidase (M4i+M5i+M6i+M9i) (Table 3). These specific glycans were identified in major amounts in the following peaks (see Table 1): FA1i in GP2, FA1iG1 in GP6, M5iA1 in GP7, M5iA2 and FM5iA1 in GP10, FM4iA1G1 in GP11, M6iA1, FA1iG1S(6)1, FM5iA1G1 and M5iA2G1 in GP15, FM5iA2G1 and M6iA1G1 in GP17, M5iA2G2 and FM4iA1G1S(6)1 in GP18, FM6iA1G1 and M5iA1G1S(6)1 in GP19, FM5iA1G1S(6)1 and M5iA2G1S(6)1 in GP21, FM5iA2G1S(6)1 in GP22, and FM5iA2G2S(6)1 in GP26. The specific glycans were also present in minor amounts in the following peaks (see Table 1): FM4i in GP4, M4iA1G1 in GP8, M6iA1, FM5iA2 and M5iA1G1 in GP13, M4A1G1S(6)1 in GP16, FM5iA2G2 in GP20, and M9i in GP23. MAN1B1-CDG-specific isomer (mannose not cleaved) of normal mannosylated glycans is indicated by i.

Table 3. Sum of Specific IgG MAN1B1-CDG *N*-Glycans for All Samples[a]

patient	percent area of unique *N*-glycans
control	1.62
1	33.16
2.1	31.75
2.2	4.04
3	9.19
4	29.93
5	37.18
6.1	33.76
6.2	25.93
7	32.29
8	31.74

[a]The percent areas were calculated from ABS+BTG (FA1i) and ABS+BTG+BKF+GUH (all Mi = M4i+M5i+M6i+M9i) digests (best separation for quantification). Percent area of unique MAN1B1-CDG *N*-glycans= FA1i+M4i+M5i+M6i+M9i (Figure 3).

N-Glycan Profiles of Total Serum Glycoproteins from MAN1B1-CDG Patients

Our updated version of high-throughput *N*-glycan analysis platform was utilized for serum glycan analysis.[13] The *N*-glycan pool released from serum was separated into 46 peaks and assigned based on Saldova et al.[17] and exoglycosidase digests (Figure 4A, Table 4).

Figure 4B shows *N*-glycan pools from all patients compared to that of the healthy control. The most significant observation is an increase in high mannose glycans in all patients except for patient 2.2 and an increase in glycans containing the sLex epitope (triantennary trigalactosylated outer arm fucosylated trisialylated glycans, Figure 5) in all patients (Figure 4B, Table 5) compared to the healthy control. Also, there seems to be a decrease in simple glycans at the beginning of the profile and an increase in highly branched and sialylated glycans at the end of the profile in patients compared to those of the healthy control (Table 5).

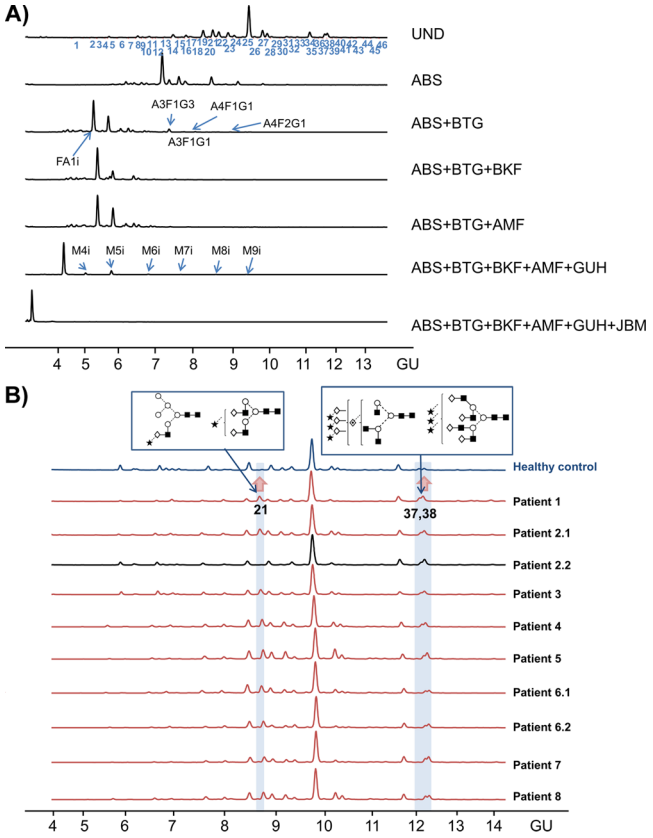

Figure 4. (A) Exoglycosidase digestions of the total *N*-linked glycan pool of serum isolated from patient 8. Specific glycans for MAN1B1-CDG and sLex epitope-containing glycans are highlighted. (B) HILIC-UPLC chromatograms of the total *N*-linked glycan pool of serum from all patients. The healthy control sample was obtained from another project. Samples are colored based on similarity (control in blue, patients more similar to control—at the beginning of the profile—are in black, and patients from the two sets similar to each other are in red). Significantly increased peaks are highlighted and their composition is in Table 4. Major glycans in affected peaks are highlighted

MAN1B1-CDG specific glycans were quantified by digestion of the glycan pool with sialidase and β-galactosidase and with sialidase, β-galactosidase, bovine kidney α-fucosidase, and β-*N*-acetylglucosaminidase. The total was calculated from the sum of specific glycans after digestion with sialidase and β-galactosidase (digest FA1i) and specific glycans after sialidase, β-galactosidase, bovine kidney α-fucosidase, and β-*N*-acetylglucosaminidase (M4i+M5i+M6i+M7i+M8i+M9). All patients except for patient 2.2 have significantly higher amounts of the MAN1B1-CDG-specific glycans compared to those of the healthy control (Table 6, quantified after exoglycosidase digestion).

SLe*x*-containing glycans were separated and quantified after digesting the glycan pool with sialidase and β-galactosidase. After the digestions, the sialylated α(1,3)-fucosylated triantennary and tetraantennary sialylated structures formed the α(1,3)-fucosylated monogalactosylated triantennary structure (A3F1G1),

DOI: 10.1021/acs.jproteome.5b00709
J. Proteome Res. 2015, 14, 4402−4412

Table 4. Predominant *N*-Glycans in 46 Peaks in CDG Serum Samples

Peak	Name	Structure	GU
GP1	A1		4.81
GP2	FA1		5.24
GP3	A1[6]G1		5.33
GP4	A2B		5.60
GP5	FA2		5.82
GP6	M5		6.14
GP7	A2[6]BG1		6.51
GP8	FA2[6]G1		6.64
GP9	FA2[3]G1		6.76
GP10	FA2[6]BG1		6.93
GP11	M6 D3		7.04
GP12	A1[3]G1S[3]1		7.16
	A2G2		
GP13	A2BG2		7.32
GP14	FA2G2		7.53
GP15	FA2BG2		7.73
GP16	A2[3]BG1S1		7.93
GP17	FA2[3]G1S1		8.01
GP18	FA2[3]BG1S[3]1		8.17
GP19	A2G2S[6]1		8.36
GP20	A2BG2S[6]1		8.52
GP21	M5A1G1S[3]1		8.62
	A2G2S[3]1		
GP22	FA2G2S1		8.77
GP23	FA2BG2S1	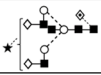	9.02
GP24	A2G2S[3,6]2		9.24

Peak	Name	Structure	GU
GP25	A2G2S[3,6]2		9.66
GP26	A2BG2S[3,6]2		9.83
GP27	FA2G2S[3,6]2		10.07
GP28	FA2BG2S[6,6]2		10.23
GP29	A3G3S[3,6]2		10.35
GP30	A4G4S[3]1		10.65
GP31	A3G3S[3,3]2		10.83
GP32	A3G3S[3,3,3]3		10.99
GP33	A3G3S[3,3,6]3		11.20
GP34	A3G3S[3,3,6]3		11.61
GP35	A3BG3S[3,3,3]3		11.75
GP36	FA3G3S[3,6,6]3		11.95
GP37	A3F1G3S[3,3,3]3		12.12
GP38	A4G4S[3,3,3]3		12.19
GP39	A4G4S[3,3,6]3		12.38
	A4G4S[3,6,6]3		
GP40	A4F1G3S[3,3,3]3		12.50
	A4F1G3S[3,3,6]3		
	A4F1G3S[3,3,6]3		
GP41	A4G4S[3,3,3,3]4		12.81
GP42	A4G4S[3,3,3,6]4		13.03
GP43	A4G4S[3,3,3,6]4		13.35
GP44	A4G4S[3,3,3,3]4		13.50
GP45	A4F1G4S[3,3,3,6]4		13.88
GP46	A4F3G4S[3,3,3,3]4		14.32

DOI: 10.1021/acs.jproteome.5b00709
J. Proteome Res. 2015, 14, 4402−4412

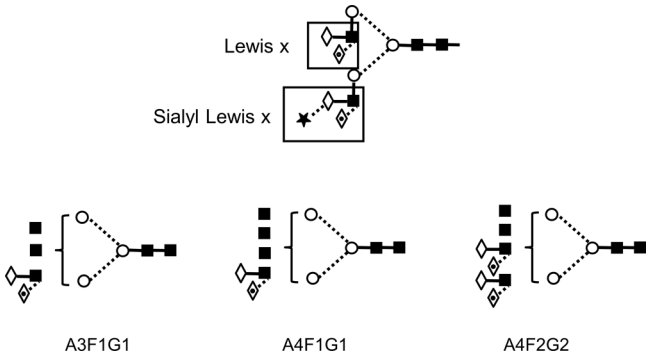

Figure 5. Illustration of Lewis *x* and sialyl Lewis *x* epitopes and the digestion products of serum glycans containing these epitopes after digestion with sialidase and β-galactosidase.

α(1,3)-fucosylated monogalactosylated tetraantennary structure (A4F1G1), and α(1,3)-difucosylated digalactosylated tetraantennary structure (A4F2G2). These digestion products elute as clear baseline-separated peaks, allowing accurate quantification by the percent area under each peak (Figure 4A). Total sLe*x* is the sum of the three peaks that contain the sLe*x* epitope (A3F1G1+A4F1G1+A4F2G2) (Table 6). The glycans containing sLe*x* epitopes were increased in all patients compared to healthy controls (Table 6).

DISCUSSION

The present paper focuses on a detailed characterization of the full repertoire of MAN1B1 glycans on serum IgG and serum glycoproteins and extends these findings to the identification of glycan abnormalities beyond the direct functional loss of MAN1B1 deficiency. These patients were analyzed by Rymen et al.[8] and Van Scherpenzeel et al.,[5] who found MAN1B1-CDG-specific glycans (hybrid, high mannosylated glycans) both on serum glycoproteins and isolated IgG. Namely, Rymen et al. found accumulation of M5A1G1S1, FM5A1G1S1, M4A1G1S1, FM4A1G1S1, and M6 in serum of MAN1B1-CDG patients.[8] Van Scherpenzeel et al. found M4A1G1S1 and M5A1G1S1 in transferrin, M6, M4A1G1S1, M5A1G1S1, and FM5A1G1S1 on serum glycoproteins, and hybrid-type high mannose glycans in IgG and alpha1-antitrypsin.[5] In addition, we have identified other specific IgG glycosylation abnormalities typical for MAN1B1-CDG using our high-throughput quantitative and sensitive technique (Table 1). The abnormal glycans contain high mannosylated hybrid glycans, mostly penta- and hexamannosylated glycans with one or two antennas and one or two galactose residues; some are monosialylated (Table 1). We have quantified the total amounts of the specific MAN1B1-CDG-specific glycoforms in both serum and IgG in all patients (Tables 2 and 5). The patterns of two patients, 2.2 and 3, are comparable to that of the control profile (Figure 3B and Table 3).

Previously unreported MAN1B1-CDG structures found in the present study highlight the sensitivity and high-resolution of the UPLC-HILIC technology. Matrix-assisted laser desorption/ionization (MALDI) mass spectrometry used in Rymen et al.[8] and Van Scherpenzeel et al.[5] is a different technique; furthermore, selection of the structures depends on a search of specific masses corresponding to glycans, whereas with the UPLC-HILIC technique, the glycans are fluorescently labeled and therefore all visible in the spectra.

We have also found an increase in sLe*x*-containing glycans in sera of all patients. This has not been reported before in MAN1B1 or any other CDG (Figure 4B, Table 6). An increase in the sLe*x* epitope has been found on acute phase proteins in inflammation and cancer.[18] This may possibly indicate that MAN1B1-CDG is associated with some inflammatory activity, although infections/inflammations are not part of these patients' phenotype. The reason for the increase in sLe*x* may be a disruption of Golgi morphology in these patients. Golgi pH is dysregulated in cancer and interestingly, also in another CDG-II, ATP6 V0A2-CDG.[19] Altered Golgi morphology in MAN1B1-CDG may lead to dysregulation of Golgi pH leading to glycosylation defects, including the presence of the sLe*x* epitope. Some glycosylation events are sensitive to Golgi pH changes, such as α(2,3)-sialylation, which is affected by a slight Golgi pH increase.[19] The increased level of sLe*x* glycans (containing α(2,3)-sialic acid) in MAN1B1 patients may originate in disruption of Golgi morphology in these patients.

Glycans play various biological roles on glycoproteins, e.g., in protein folding, trafficking, ligand recognition, biological activity, stability, and regulating protein half-life and immunogenicity.[20] Glycosylation on immunoglobulin G has a significant impact on immune function. The absence of core fucose and the presence of bisecting GlcNAc on IgG enhances antibody-dependent cell-mediated cytotoxicity (ADCC) activity,[21,22] whereas sialic acid on IgG suppresses ADCC activity.[23] Galactose is important for placental transport.[24] GlcNAc and mannose are ligands for mannose binding lectin and enhance complement-dependent cytotoxicity (CDC).[25] IgG glycans also have a significant impact on binding to FcγR and the subsequent immune responses.[26]

Sialic acids are also biologically important, not only in quantity, but also the structure, linkage, class, and spatial organization.[27,28] Siglecs are immunoglobulin-like lectins binding sialic acids, and they are involved in cell−cell interactions and signaling functions in the hemopoietic, immune, and nervous systems in signaling and adhesion[29] and are species-specific.[28] They are important in host-defense because sialic acids are species-specific and absent from many pathogens.[29] The pathogens either synthesize or acquire sialic acids from the host and use siglecs to manipulate the host immune response.[30] The virulent parasite *Leishmania sp.* contains higher amounts of sialic acids.[31] Modification of sialic acids, such as *O*-acetylation, also play a role in its virulence.[31] α(2,6)-Sialylation mediates tumor progression via enhanced β1-integrin function and is associated with poor prognosis.[32] Sialic acids have important roles in immunity, such as modulation of leukocyte trafficking via selectins, ligands for microbes, pathogen molecular mimicry of host sialic acids, polysialic acid modulation of immune cells, modulation of immunity by sialic acid *O*-acetylation, as antigens and xeno-autoantigens, antisialoglycan antibodies in reproductive incompatibility, and sialic acid-based blood groups.[33] sLe*x* is a key component of sialylated selectin ligands and of preferred ligands for some siglecs.[33]

These findings, i.e., the increase in MAN1B1-CDG specific and sLe*x* glycans, could lead to disruption of a wide range of body systems leading to these patients' phenotypes.

In summary, our work has demonstrated specific glycan abnormalities for MAN1B1-CDG, partially corresponding with the deficient enzymatic activity of Golgi α(1,2)-mannosidase, but additional observed glycan structures are possibly related to other functions of MAN1B1.

DOI: 10.1021/acs.jproteome.5b00709
J. Proteome Res. 2015, 14, 4402−4412

Table 5. Percent Areas of 46 Peaks in CDG Serum Samples[a]

sample	GP1	GP2	GP3	GP4	GP5	GP6	GP7	GP8	GP9	GP10	GP11
control	0.07	0.13	0.03	0.22	4.02	2.19	0.16	4.05	1.69	1.24	1.23
1	0.08	**0.03**	*0.12*	**0.07**	**0.81**	**0.74**	**0.02**	**0.99**	**0.29**	2.24	**0.55**
2.1	0.08	0.17	0.02	**0.06**	**0.84**	**0.74**	**0.05**	**1.53**	**0.42**	1.87	**0.57**
2.2	0.04	**0.03**	*0.07*	**0.04**	3.17	1.66	**0.08**	2.94	**0.84**	0.72	0.95
3	0.04	**0.07**	*0.06*	**0.06**	2.55	**0.99**	**0.07**	3.35	1.12	1.99	0.78
4	0.07	0.18	0.05	**0.04**	**1.14**	**0.68**	0.09	**1.29**	**0.48**	1.85	**0.37**
5	0.03	**0.05**	0.04	**0.01**	**0.40**	**0.24**	**0.06**	**0.93**	**0.34**	0.87	**0.19**
6.1	0.04	**0.07**	0.04	**0.03**	**0.53**	**0.43**	0.09	**0.95**	**0.30**	1.65	**0.29**
6.2	0.05	**0.07**	0.04	**0.03**	**0.54**	**0.34**	**0.08**	**0.78**	**0.23**	1.51	**0.26**
7	0.02	**0.03**	0.02	**0.01**	**0.24**	**0.21**	**0.05**	**0.64**	**0.18**	0.89	**0.19**
8	0.04	**0.07**	0.03	**0.02**	**0.60**	**0.29**	**0.06**	**1.05**	**0.36**	0.99	**0.20**

sample	GP12	GP13	GP14	GP15	GP16	GP17	GP18	GP19	GP20	GP21
control	0.51	**0.10**	**3.95**	**0.62**	1.08	**0.73**	0.05	**7.62**	**0.21**	0.67
1	0.40	*0.24*	**1.63**	0.66	1.97	0.44	*0.22*	**3.11**	0.25	*6.17*
2.1	0.31	*0.25*	2.68	0.78	1.95	0.68	*0.22*	4.98	0.24	*6.88*
2.2	0.43	**0.04**	2.51	0.29	1.17	0.51	0.05	4.92	0.13	0.38
3	0.38	0.15	2.83	0.88	1.93	0.48	*0.18*	4.84	0.24	*5.95*
4	0.74	*0.70*	2.68	1.11	*2.34*	1.43	*0.30*	6.61	*0.90*	*6.91*
5	0.48	*0.42*	2.95	0.78	1.95	1.29	*0.21*	6.74	*0.70*	*7.39*
6.1	0.67	*0.67*	2.82	1.02	*2.50*	1.21	*0.34*	8.50	*0.98*	*7.36*
6.2	0.68	*0.63*	**1.91**	1.02	*2.33*	1.00	*0.29*	7.49	*1.06*	*7.57*
7	0.51	*0.43*	2.16	0.75	1.99	0.88	*0.19*	6.10	*0.86*	*6.55*
8	0.49	*0.54*	2.79	0.81	1.99	1.40	*0.28*	6.27	*0.85*	*6.64*

sample	GP22	GP23	GP24	GP25	GP26	GP27	GP28	GP29	GP30	GP31
control	**5.45**	**2.24**	4.39	32.63	1.32	**4.18**	**2.23**	**1.39**	**0.12**	**0.69**
1	**2.45**	2.22	3.25	37.05	0.90	2.58	**0.68**	0.85	0.10	0.43
2.1	4.47	3.59	3.11	33.85	1.25	4.64	2.96	0.97	0.06	0.67
2.2	4.75	**0.82**	4.66	37.98	0.99	3.38	0.70	1.02	0.07	0.61
3	3.82	2.46	3.08	36.52	1.04	4.00	1.86	0.76	0.08	0.48
4	5.24	5.30	2.60	29.74	0.79	4.91	2.47	1.40	*0.28*	0.89
5	6.59	*6.58*	**2.01**	25.44	0.93	8.48	3.18	1.47	*0.29*	0.96
6.1	6.47	4.20	2.86	31.84	0.93	4.24	1.76	1.57	*0.30*	1.12
6.2	4.52	3.35	3.63	35.59	0.88	2.98	**1.01**	1.66	*0.32*	1.01
7	4.95	3.42	2.90	33.29	0.91	3.11	**0.88**	1.64	*0.49*	1.06
8	6.27	*5.23*	**2.11**	27.96	1.04	6.80	3.60	1.49	*0.30*	1.17

sample	GP32	GP33	GP34	GP35	GP36	GP37	GP38	GP39	GP40	GP41
control	**0.27**	**0.80**	*6.21*	0.30	0.46	*1.62*	*2.43*	0.30	0.27	*0.80*
1	*0.51*	0.61	6.95	0.44	0.32	*3.28*	*7.12*	0.41	*0.50*	*0.79*
2.1	0.33	0.59	5.63	0.32	**0.22**	2.00	*5.43*	0.27	0.30	0.46
2.2	0.39	0.93	7.26	*0.60*	0.45	1.91	*7.76*	0.38	*0.62*	0.44
3	0.36	0.40	4.07	0.29	**0.22**	1.54	4.67	0.34	0.35	0.57
4	*0.89*	0.85	4.92	0.45	0.41	2.29	3.82	0.41	*0.43*	0.42
5	*1.05*	0.84	4.62	0.49	0.50	2.00	*4.89*	*0.62*	*0.66*	0.56
6.1	*0.74*	0.82	5.10	0.34	0.33	1.98	*2.80*	0.31	0.29	0.38
6.2	*0.91*	0.98	5.64	0.56	0.30	2.04	4.20	0.32	0.38	0.43
7	*1.20*	1.15	6.93	*0.63*	0.36	3.46	*6.16*	0.49	*0.50*	*0.71*
8	*0.86*	0.92	5.53	0.41	0.47	2.95	3.90	*0.61*	*0.45*	0.50

sample	GP42	GP43	GP44	GP45	GP46
control	0.47	0.56	0.26	0.28	0.23
1	*1.01*	*1.61*	*1.33*	*2.19*	*1.53*
2.1	0.56	0.86	*0.61*	*0.95*	*0.67*
2.2	0.56	0.74	*0.59*	*0.89*	*0.66*
3	0.56	0.98	*0.66*	*1.13*	*0.92*
4	0.26	0.43	0.26	0.37	0.20
5	0.27	0.47	0.30	*0.44*	0.28
6.1	**0.21**	0.36	0.19	0.24	0.13
6.2	0.27	0.42	0.24	0.33	0.17
7	0.47	0.73	*0.50*	*0.73*	*0.44*
8	0.26	0.48	0.28	0.40	0.25

[a]Italics indicate more than 100% increase, and bold indicates more than 100% decrease in percent area of peaks in patients compared to healthy controls.

DOI: 10.1021/acs.jproteome.5b00709
J. Proteome Res. 2015, 14, 4402−4412

Table 6. Sum of Specific MAN1B1 Serum CDG *N*-Glycans for All Samples

patient	percentage area of unique *N*-glycans[a]	total sLe*x*[b]
healthy control	1.95	2.77
1	17.01	7.97
2.1	18.36	7.29
2.2	0.81	9.40
3	12.20	6.11
4	20.90	5.67
5	19.19	6.93
6.1	20.39	4.12
6.2	17.91	6.02
7	16.38	8.51
8	18.19	4.78

[a]Percent areas of MAN1B1-CDG-specific glycans were calculated from ABS+BTG (FA1i) and ABS+BTG+BKF+GUH (all Mi = M4i+M5i+M6i+M7i+M8i+M9i) digests (best separation for quantification). Percent areas of unique MAN1B1 *N*-glycans = FA1i+M4i+M5i+M6i+M7i+M8i+M9i (Figure 4A). [b]Percent areas of sLe*x*-containing glycans were calculated from ABS+BTG (A3F1G1+A4F1G1+A4F2G2), and total sLe*x*-containing glycans sum them (Figure 4A).

■ ASSOCIATED CONTENT

Supporting Information

The Supporting Information is available free of charge on the ACS Publications website at DOI: 10.1021/acs.jproteome.5b00709.

Updated version of the automated serum glycomics platform (PDF)

Phenotype and genotype of the MAN1B1-CDG patients (PDF)

■ AUTHOR INFORMATION

Corresponding Author

*Phone: (+353) 1215 8142. Fax: (+353) 1215 8116. E-mail: pauline.rudd@nibrt.ie.

Notes

The authors declare no competing financial interest.

■ ACKNOWLEDGMENTS

The authors would like to thank Dr. Mohan Muniyappa for help with isolation of IgG from control serum on the robotic platform. R.S. acknowledges funding from the European Union Seventh Framework Programme (FP7/2007-2013) under grant agreement No. 260600 ("GlycoHIT") and funding from the Science Foundation Ireland Starting Investigator Research grant (SFI SIRG) under Grant Number 13/SIRG/2164. H.S. and R.O.F. acknowledge funding from EU FP7 program HighGlycan, Grant No. 278535. D.L acknowledges funding by the Dutch Organisation for Scientific Research, NWO (Medium Investment Grant 40-00506-98-9001).

■ REFERENCES

(1) Marino, K.; Saldova, R.; Adamczyk, B.; Rudd, P. M. Changes in serum *N*-glycosylation profiles: functional significance and potential for diagnostics. In *Carbohydrate Chemistry: Chemical and Biological Approaches*; Rauter, A. P., Ed.; RSC Publishing, 2012; Vol. 37, pp 57–93.

(2) Rudd, P. M.; Elliott, T.; Cresswell, P.; Wilson, I. A.; Dwek, R. A. Glycosylation and the immune system. *Science* **2001**, *291*, 2370–6.

(3) Arnold, J. N.; Wormald, M. R.; Sim, R. B.; Rudd, P. M.; Dwek, R. A. The impact of glycosylation on the biological function and structure of human immunoglobulins. *Annu. Rev. Immunol.* **2007**, *25*, 21–50.

(4) Barone, R.; Fiumara, A.; Jaeken, J. Congenital disorders of glycosylation with emphasis on cerebellar involvement. *Semin Neurol* **2014**, *34*, 357–66.

(5) Van Scherpenzeel, M.; Timal, S.; Rymen, D.; Hoischen, A.; Wuhrer, M.; Hipgrave-Ederveen, A.; Grunewald, S.; Peanne, R.; Saada, A.; Edvardson, S.; Gronborg, S.; Ruijter, G.; Kattentidt-Mouravieva, A.; Brum, J. M.; Freckmann, M. L.; Tomkins, S.; Jalan, A.; Prochazkova, D.; Ondruskova, N.; Hansikova, H.; Willemsen, M. A.; Hensbergen, P. J.; Matthijs, G.; Wevers, R. A.; Veltman, J. A.; Morava, E.; Lefeber, D. J. Diagnostic serum glycosylation profile in patients with intellectual disability as a result of MAN1B1 deficiency. *Brain* **2014**, *137*, 1030–8.

(6) Freeze, H. H. Genetic defects in the human glycome. *Nat. Rev. Genet.* **2006**, *7*, 537–51.

(7) Jakob, C. A.; Burda, P.; Roth, J.; Aebi, M. Degradation of misfolded endoplasmic reticulum glycoproteins in Saccharomyces cerevisiae is determined by a specific oligosaccharide structure. *J. Cell Biol.* **1998**, *142*, 1223–33.

(8) Rymen, D.; Peanne, R.; Millon, M. B.; Race, V.; Sturiale, L.; Garozzo, D.; Mills, P.; Clayton, P.; Asteggiano, C. G.; Quelhas, D.; Cansu, A.; Martins, E.; Nassogne, M. C.; Goncalves-Rocha, M.; Topaloglu, H.; Jaeken, J.; Foulquier, F.; Matthijs, G. MAN1B1 deficiency: an unexpected CDG-II. *PLoS Genet.* **2013**, *9*, e1003989.

(9) Rafiq, M. A.; Kuss, A. W.; Puettmann, L.; Noor, A.; Ramiah, A.; Ali, G.; Hu, H.; Kerio, N. A.; Xiang, Y.; Garshasbi, M.; Khan, M. A.; Ishak, G. E.; Weksberg, R.; Ullmann, R.; Tzschach, A.; Kahrizi, K.; Mahmood, K.; Naeem, F.; Ayub, M.; Moremen, K. W.; Vincent, J. B.; Ropers, H. H.; Ansar, M.; Najmabadi, H. Mutations in the alpha 1,2-mannosidase gene, MAN1B1, cause autosomal-recessive intellectual disability. *Am. J. Hum. Genet.* **2011**, *89*, 176–82.

(10) Royle, L.; Campbell, M. P.; Radcliffe, C. M.; White, D. M.; Harvey, D. J.; Abrahams, J. L.; Kim, Y. G.; Henry, G. W.; Shadick, N. A.; Weinblatt, M. E.; Lee, D. M.; Rudd, P. M.; Dwek, R. A. HPLC-based analysis of serum N-glycans on a 96-well plate platform with dedicated database software. *Anal. Biochem.* **2008**, *376*, 1–12.

(11) Marino, K.; Bones, J.; Kattla, J. J.; Rudd, P. M. A systematic approach to protein glycosylation analysis: a path through the maze. *Nat. Chem. Biol.* **2010**, *6*, 713–23.

(12) Stöckmann, H.; Adamczyk, B.; Hayes, J.; Rudd, P. M. Automated, high-throughput IgG-antibody glycoprofiling platform. *Anal. Chem.* **2013**, *85*, 8841–9.

(13) Stöckmann, H.; O'Flaherty, R.; Adamczyk, B.; Saldova, R.; Rudd, P. M. Automated, high-throughput serum glycoprofiling platform. *Integr Biol. (Camb)* **2015**, *7*, 1026–32.

(14) Bigge, J. C.; Patel, T. P.; Bruce, J. A.; Goulding, P. N.; Charles, S. M.; Parekh, R. B. Nonselective and efficient fluorescent labeling of glycans using 2-amino benzamide and anthranilic acid. *Anal. Biochem.* **1995**, *230*, 229–38.

(15) Royle, L.; Radcliffe, C. M.; Dwek, R. A.; Rudd, P. M. Detailed structural analysis of N-glycans released from glycoproteins in SDS-PAGE gel bands using HPLC combined with exoglycosidase array digestions. *Methods Mol. Biol.* **2006**, *347*, 125–43.

(16) Pucic, M.; Knezevic, A.; Vidic, J.; Adamczyk, B.; Novokmet, M.; Polasek, O.; Gornik, O.; Supraha-Goreta, S.; Wormald, M. R.; Redzic, I.; Campbell, H.; Wright, A.; Hastie, N. D.; Wilson, J. F.; Rudan, I.; Wuhrer, M.; Rudd, P. M.; Josic, D.; Lauc, G. High throughput isolation and glycosylation analysis of IgG-variability and heritability of the IgG glycome in three isolated human populations. *Mol. Cell. Proteomics* **2011**, *10*, M111.010090.

(17) Saldova, R.; Asadi Shehni, A.; Haakensen, V. D.; Steinfeld, I.; Hilliard, M.; Kifer, I.; Helland, A.; Yakhini, Z.; Borresen-Dale, A. L.; Rudd, P. M. Association of N-glycosylation with breast carcinoma and systemic features using high-resolution quantitative UPLC. *J. Proteome Res.* **2014**, *13*, 2314–27.

(18) Saldova, R.; Wormald, M. R.; Dwek, R. A.; Rudd, P. M. Glycosylation changes on serum glycoproteins in ovarian cancer may contribute to disease pathogenesis. *Dis. Markers* **2008**, *25*, 219–32.

DOI: 10.1021/acs.jproteome.5b00709
J. Proteome Res. 2015, 14, 4402–4412

(19) Rivinoja, A.; Pujol, F. M.; Hassinen, A.; Kellokumpu, S. Golgi pH, its regulation and roles in human disease. *Ann. Med.* **2012**, *44*, 542−54.
(20) Brooks, S. A.; Dwek, M. W.; Schumacher, U. *Functional & Molecular Glycobiology*; BIOS Scientific Publishers Limited: Oxford, 2002.
(21) Okazaki, A.; Shoji-Hosaka, E.; Nakamura, K.; Wakitani, M.; Uchida, K.; Kakita, S.; Tsumoto, K.; Kumagai, I.; Shitara, K. Fucose depletion from human IgG1 oligosaccharide enhances binding enthalpy and association rate between IgG1 and FcgammaRIIIa. *J. Mol. Biol.* **2004**, *336*, 1239−49.
(22) Umana, P.; Jean-Mairet, J.; Moudry, R.; Amstutz, H.; Bailey, J. E. Engineered glycoforms of an antineuroblastoma IgG1 with optimized antibody-dependent cellular cytotoxic activity. *Nat. Biotechnol.* **1999**, *17*, 176−80.
(23) Kaneko, Y.; Nimmerjahn, F.; Ravetch, J. V. Anti-inflammatory activity of immunoglobulin G resulting from Fc sialylation. *Science* **2006**, *313*, 670−3.
(24) Kibe, T.; Fujimoto, S.; Ishida, C.; Togari, H.; Okada, S.; Nakagawa, H.; Tsukamoto, Y.; Takahashi, N. Glycosylation and placental transport of IgG. *J. Clin. Biochem. Nutr.* **1996**, *21*, 57−63.
(25) Malhotra, R.; Wormald, M. R.; Rudd, P. M.; Fischer, P. B.; Dwek, R. A.; Sim, R. B. Glycosylation changes of IgG associated with rheumatoid arthritis can activate complement via the mannose-binding protein. *Nat. Med.* **1995**, *1*, 237−43.
(26) Hayes, J. M.; Cosgrave, E. F.; Struwe, W. B.; Wormald, M.; Davey, G. P.; Jefferis, R.; Rudd, P. M. Glycosylation and Fc receptors. *Curr. Top. Microbiol. Immunol.* **2014**, *382*, 165−99.
(27) Cohen, M.; Varki, A. The sialome–far more than the sum of its parts. *OMICS* **2010**, *14*, 455−64.
(28) Crocker, P. R. Siglecs in innate immunity. *Curr. Opin. Pharmacol.* **2005**, *5*, 431−7.
(29) Crocker, P. R. Siglecs: sialic-acid-binding immunoglobulin-like lectins in cell-cell interactions and signalling. *Curr. Opin. Struct. Biol.* **2002**, *12*, 609−15.
(30) Khatua, B.; Roy, S.; Mandal, C. Sialic acids siglec interaction: a unique strategy to circumvent innate immune response by pathogens. *Indian J. Med. Res.* **2013**, *138*, 648−662.
(31) Ghoshal, A.; Mandal, C. A perspective on the emergence of sialic acids as potent determinants affecting leishmania biology. *Mol. Biol. Int.* **2011**, *2011*, 532106.
(32) Hedlund, M.; Ng, E.; Varki, A.; Varki, N. M. alpha 2−6-Linked sialic acids on N-glycans modulate carcinoma differentiation in vivo. *Cancer Res.* **2008**, *68*, 388−94.
(33) Varki, A.; Gagneux, P. Multifarious roles of sialic acids in immunity. *Ann. N. Y. Acad. Sci.* **2012**, *1253*, 16−36.

DOI: 10.1021/acs.jproteome.5b00709
J. Proteome Res. 2015, 14, 4402−4412